

How Significantly do Land Use and Land Cover (LULC) Changes Influence the Water Balance of a River Basin? A Study in Ganga River Basin, India

N. Patidar^{1,3} · M. D. Behera²

Received: 23 February 2016/Revised: 30 August 2017/Accepted: 17 October 2017/Published online: 10 February 2018
© The National Academy of Sciences, India 2018

Abstract Changes in LULC, primarily conversion of natural vegetation to built-up and agricultural areas, has been one of the key modes of human modification of the global environment. Assessment of the consequences of these changes for hydrological processes is vital for sustainable management of water resources. In this study, the impacts of land use and land cover (LULC) changes on the evapotranspiration (ET) and runoff in the Ganga river basin, India during the period of 1975–2010 are assessed. Variable infiltration capacity (VIC), a physically distributed macro-scale hydrological model, is used with a grid cell resolution of 0.125° with a daily time step to simulate hydrological fluxes. The moderate resolution imaging spectroradiometer (MODIS) LAI product MCD15A3 is used to extract monthly LULC class-wise leaf area index values to parameterize the VIC model. The results indicate that the VIC model is a powerful model for assessing the hydrologic impacts of LULC change. The Nash–Sutcliffe efficiencies for the monthly stream flow were 0.650 and 0.565 during calibration and 0.764 during validation, respectively. Single-cell model simulations show that expansion of the built-up area at the cost of vegetation is the change that affected the water balance of the study area

most significantly. The effects of LULC changes are greatest during the monsoon. However, during the dry season, there are similar ET and runoff responses from most of the LULC classes because of the low soil moisture. The overall changes in the ET and runoff due to LULC changes in the study area are found to be too small at the basin. We observe that at the basin scale, the negative impacts on the ET and runoff are compensated by the positive impacts.

Keywords Impacts of LULC change · VIC model · Hydrological responses · MODIS LAI

1 Introduction

Land use and land cover (LULC) changes alter the exchange of energy and water between the atmosphere and the earth's surface and affect the dynamics of the climate system [1, 2]. Rapid anthropogenic activities and climate variability have raised intense concerns about the serious effects that LULC changes may have on water, sediment fluxes, air and water quality, soil conditions and ecosystems. Rapid anthropogenic activities such as urbanization, mining and agricultural expansion have been causing land cover modifications and conversions from one land cover class to another. Assessing and predicting the consequences of LULC changes on hydrological processes helps the linkages between LULC and hydrological dynamics to be understood better [3]. LULC changes modify land surface properties, primarily the leaf area index (LAI), surface albedo and surface roughness, which influence the energy and water balance [4, 5]. The lower LAI, higher surface albedo and shallower rooting depth of non-forest classes, compared with forest classes, reduce the ET, with a

✉ N. Patidar
niteshpatidar88@gmail.com

¹ School of Water Resources, Indian Institute of Technology Kharagpur, Kharagpur 721302, India

² Spatial Analysis and Modelling Laboratory, Centre for Oceans, Rivers, Atmosphere and Land Sciences, Indian Institute of Technology Kharagpur, Kharagpur 721302, India

³ Present Address: Department of Civil Engineering, Indian Institute of Technology Delhi, Hauz Khas, New Delhi 110016, India

corresponding increase in the surface runoff. The conversion of forests to non-forest classes leads to reduced interception of water and snow, higher sediment yields through modified rates of soil erosion, and increased overland flows [6, 7]. Further, the increase in the extent of impervious surfaces that is associated with urbanization amplifies the runoff yield by preventing water from infiltrating into the ground. These can significantly affect the streamflow, frequency of floods, magnitude and timing of ET and regional and global climates [6, 8–11].

According to the literature, the magnitude of the hydrologic impacts of LULC change is greatly dependent on the size of the catchment. In general, the impacts of LULC change are more pronounced in small catchments [12]. In contrast, in a large catchment, these impacts may be relatively weaker because there may be both deforestation and afforestation at the same time, counterbalancing each other [8, 11, 13]. However, there is evidence that large-scale LULC changes may have significant hydrologic impacts in large river basins [5, 14, 15]. The hydrologic impacts of LULC changes also depend on the type and degree of LULC transformation and the climatic conditions in the catchment. Therefore, it is worthwhile to explore how significant LULC changes are in altering the water balance of a particular catchment.

The impacts of LULC changes on the hydrological components have been assessed in many river basins worldwide using conceptual and physical hydrological models [5, 10, 11, 16–23]. Conceptual models may not always be suitable for hydrologic impact studies since vegetation parameters such as the crop factor, which do not have a physical meaning, can be involved in the calibration of the model, making it difficult to differentiate LULC classes [15]. The variable infiltration capacity (VIC) model has proved to be suitable for hydrologic impact studies since it uses physical vegetation parameters, including LAI and albedo, at a monthly timescale [5, 8, 10, 21, 24]. In addition, this model allows the sub-grid heterogeneity of the LULC to be defined using fractions of LULC classes within the grid cell.

Several studies have been carried out to assess the hydrologic impacts of LULC changes in India. Mishra et al. [7] found that sub-basins having forest cover have less runoff and sediment yield compared with sub-basins with other LULC classes. Dadhwal et al. [6] investigated LULC changes and their impacts on the streamflow in the Mahanadi river basin. They found that the streamflow was significantly increased due to deforestation in the basin. Wagner et al. [11] found significant LULC changes in the catchment of the Mula and Mutha rivers. They concluded that the LULC changes led to a significant increase in the overland flow at local scale; however, they found that the impacts of these changes cancelled each other at the

catchment scale. These studies, however, do not fully explore the sensitivity of the water balance in an area with seasonally limited water availability to LULC changes.

The Ganga river basin (GRB) has experienced significant LULC changes during the past few decades. Recently, Behera et al. [25] studied the LULC changes that have taken place in the GRB during the past 35 years (1975–2010). Agriculture was found to be dominant in the basin ($\sim 73\%$), followed by deciduous forest ($\sim 10\%$) and scrubland ($\sim 5\%$). In addition, the expansion of agricultural lands and human settlements at the cost of natural vegetation was the major change in the LULC in the basin. At the same time, the extent of forest plantations in the GRB was found to have increased, which was a positive sign. Substantial transformations of the LULC were observed in the GRB, with a decrease in the natural vegetation due to deforestation and urban expansion at some places. At the same time, there was an increase in the extent of the vegetation due to plantation of forests and expansion of agricultural areas at other places in the basin. As far as the authors are aware, the hydrologic impacts of these changes in the GRB have not yet been investigated. The aim of this study is to study how significant LULC changes are altering the water balance of an area with seasonally limited water availability such as the GRB.

2 Study Area

The GRB lies between latitudes $21^{\circ}40'39''\text{N}$ and $31^{\circ}27'39''\text{N}$ and longitudes $73^{\circ}13'00''\text{E}$ and $89^{\circ}09'53''\text{E}$, draining an area of $1,086,000\text{ km}^2$ in India, Tibet, Nepal and Bangladesh. The Ganga river originates from the western Himalaya, flows through the Gangetic plain in northeast India and drains into the Bay of Bengal. The Ganga has significant economic, environmental and cultural values in India. Only the area falling in India ($\sim 804,671\text{ km}^2$) is considered in this study (hereafter referred to as IGRB) since the data sets required for implementing the model for the other parts of the basin were not available (Fig. 1a). The IGRB accounts for 26% of India's landmass, 30% of its water resources and more than 40% of its population. The elevation of IGRB ranges from 1 m, near the Bay of Bengal, to 7322 m, in the Himalaya. The climate of IGRB varies from perhumid, in the southeast, to arid, in the east [26]. The precipitation in IGRB is mainly driven by the Indian summer monsoon (June–September), and more than 70% of the annual precipitation falls during the monsoon months. The months from October to May are relatively dry. The annual average precipitation varies from 543 mm, in the west, to more than 2000 mm, in the northeast, while the average annual temperature varies from $-5\text{ }^{\circ}\text{C}$, in the north, to $27\text{ }^{\circ}\text{C}$, in

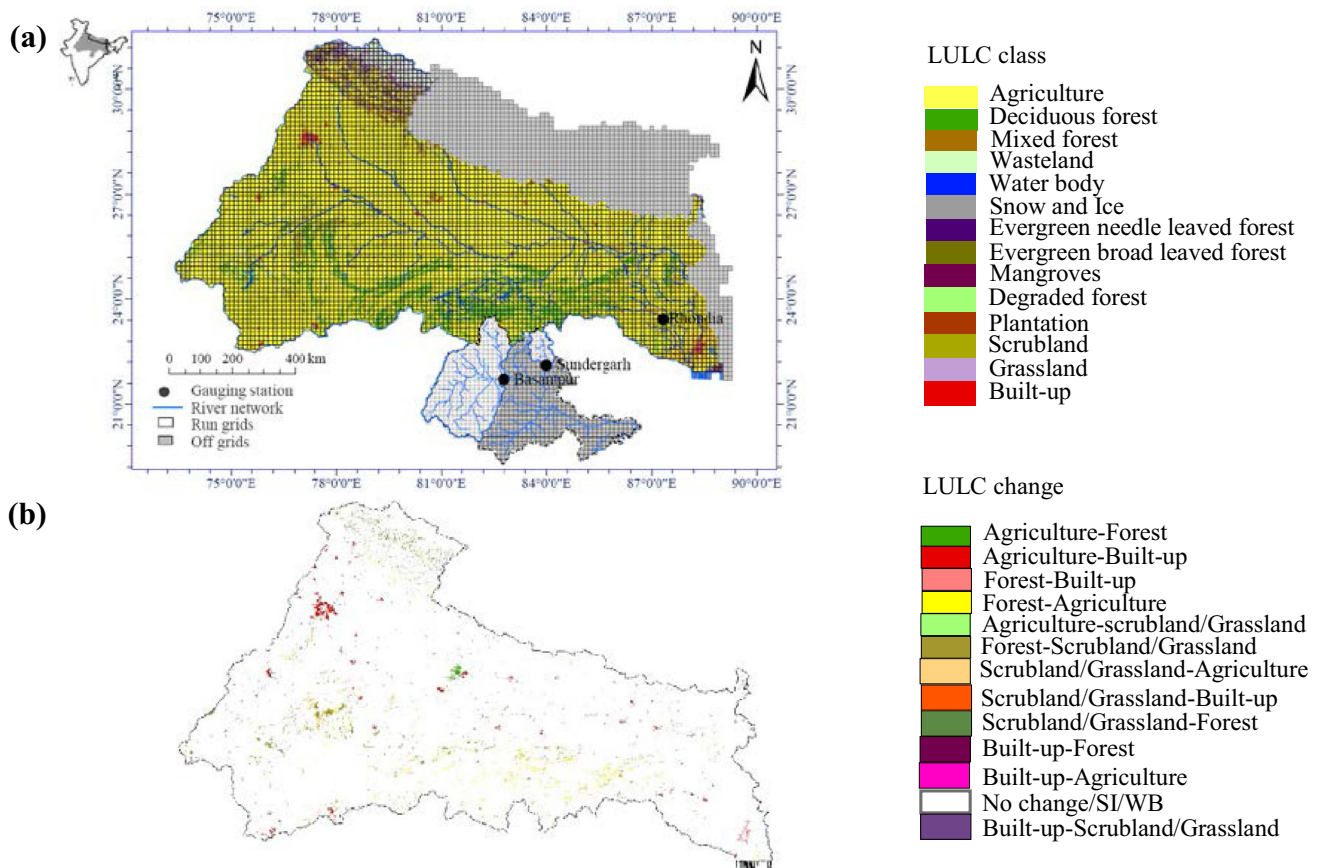


Fig. 1 Location of the study area and calibration and validation sites with distribution of LULC during the year 2010 (a), and LULC change during 1975–2010 (b). Modified after Behera et al. [25]

the east. The LULC in IGRB is dominated by agriculture, followed by deciduous forest (Fig. 1). The agricultural lands are mainly found in the Gangetic plain, with deciduous forest being found mainly in the mountainous region in the southern part of IGRB. Evergreen forest (including evergreen needle-leaved forest and evergreen broad-leaved forest) is only found in the Himalayan foothills in the northern part of IGRB.

3 Methodology

3.1 Model Description

The VIC hydrological model (version 4.2) was used to assess the hydrologic impacts of the LULC changes in IGRB. The semi-distributed VIC model was specifically developed to simulate the water and energy balances of macro-scale catchments [24, 27]. The key characteristics of the grid-based VIC model are its representation of vegetation heterogeneity, multiple soil layers with variable infiltration and non-linear base flows. To simulate a

streamflow, the results from VIC are typically post-processed with a separate routing model based on a linear transfer function [28]. The spatial variability of soil parameters and meteorological variables is considered by dividing the study domain into several square grids. The soil parameters and meteorological variables are assumed to be homogeneous within each grid cell. However, the VIC model represents vegetation heterogeneity within a grid cell using the fractional area of each vegetation type within the grid cell. The characteristics of each vegetation type are defined in the model using the monthly leaf area index (LAI) and albedo, the canopy resistance, the stomatal resistance and flags for the presence/absence of an overstorey and root zone depths.

The following analysis emphasizes how VIC simulated hydrological fluxes primarily ET and runoff are affected by changes in the LULC. The ET from each vegetation type in the VIC model is characterized using the Penman–Monteith formulation [24]. Therefore, any alteration in the vegetation parameters caused by LULC changes leads to changes in the ET and subsequently affects other water balance components such as the runoff and soil moisture.

The VIC model estimates the ET over a grid cell as the sum of the evaporation from the canopy layer of the n th vegetation tile ($E_{c,n}$), transpiration ($E_{t,n}$) from the n th vegetation tile and evaporation from the bare soil (E_j), weighted by the respective surface cover fractions [24]. The canopy evaporation from the n th vegetation tile is estimated as

$$E_{c,n} = \left(\frac{W_{i,n}}{W_{im,n}} \right)^{2/3} E_{p,n} \frac{r_{w,n}}{r_{w,n} + r_{0,n}}, \tag{1}$$

where n refers to the vegetation class index, W_{im} is the maximum amount of water the canopy can intercept (typically 0.2 times the LAI), W_i is canopy interception, r_o and r_w are the architectural and aerodynamic resistances, respectively, and E_p is the potential evapotranspiration that is calculated from the Penman–Monteith equation with the canopy resistance set to zero using meteorological variables and vegetation properties.

The transpiration from the vegetation is estimated from

$$E_{t,n} = \left(1 - \left(\frac{W_{i,n}}{W_{im,n}} \right)^{2/3} \right) E_{p,n} \frac{r_{w,n}}{r_{w,n} + r_{0,n} + r_{c,n}}, \tag{2}$$

where r_c is the canopy resistance, defined as

$$r_{c,n} = \frac{r_{0c,n} g_T g_{vpd} g_{PAR} g_{sm}}{LAI_n}, \tag{3}$$

where r_{0c} is the minimum canopy resistance and g_T , g_{vpd} , g_{PAR} and g_{sm} are the temperature factor, vapour pressure deficit factor, photosynthetically active radiation flux (PAR) factor, and soil moisture factor, respectively, each with a minimum value of 1. g_{sm} is estimated from

$$\left. \begin{aligned} \frac{1}{g_{sm}} &= 0, & \theta &\leq \theta_{wp}, \\ \frac{1}{g_{sm}} &= \frac{\theta - \theta_{wp}}{\theta^* - \theta_{wp}}, & \theta_{wp} < \theta &\leq \theta^*, \\ \frac{1}{g_{sm}} &= 1, & \theta^* < \theta &\leq \theta_s, \end{aligned} \right\} \tag{4}$$

where θ is the average soil moisture content, θ_{wp} is the plant wilting point and θ^* is the moisture content above which the soil conditions do not limit transpiration. The g_T , g_{vpd} , g_{PAR} are estimated based on temperature, vapour pressure deficit and photosynthetically active radiation flux, respectively. The details of how g_T , g_{vpd} and g_{PAR} are estimated can be found in Dickinson et al. [29]. The bare soil evaporation (E_j) is mainly governed by the soil moisture conditions. The bare soil evaporation is equal to the potential evaporation rate when the surface soil is saturated. When the top soil layer is not saturated, its evaporation rate is calculated using the Arno formulation [30].

The monthly changes in the vegetation properties are captured using the monthly LAI, albedo and vegetation height within the VIC model, whereas these monthly values are kept constant in multi-year simulations [5, 27]. The

VIC model simulates the hydrological fluxes of each grid cell individually, and therefore the water balance of a grid cell does not affect the water balance of the neighbouring grid cell during a VIC simulation. However, the grids are interconnected during the post-processing step, i.e., routing of the VIC-simulated runoff to the basin outlet using the routing module [28]. This feature of VIC allows simulation within political boundaries or hydrological units such as watersheds [31]. Therefore the VIC model is suitable for analysing the hydrologic impacts of LULC changes in IGRB.

3.2 Model Implementation

The VIC simulations were performed at a 1/8° grid resolution with a daily time step. The grids are typically classified into two categories, run grids and off grids. Simulations are performed only for the run grids, while the off grids are skipped during a simulation. In the present study, grids falling in IGRB were assigned as run grids, and the remaining grids of GRB were considered as off grids (Fig. 1a). The three types of input data to be defined to implement the VIC model are vegetation properties, soil properties and time-series of meteorological data.

The soil parameters were defined using a soil texture map acquired from the National Bureau of Soil Survey and Land Use Planning (NBSS and LUP), India. Two soil layers were defined, with depths of 0.3 and 0.7 m, respectively. The hydraulic properties of each soil texture, such as the saturated hydraulic conductivity, porosity, field capacity and wilting point, were derived using the soil hydraulic properties index of Cosby et al. [32]. Soil parameters including the variable infiltration curve parameter (b_i), fraction of maximum velocity of base flow where non-linear base flow begins (D_s), fraction of maximum soil moisture where non-linear base flow occurs (W_s) and soil layer thicknesses (D_1 and D_2) were adjusted during the calibration phase.

The vegetation properties were defined on the basis of the LULC maps of 1975 and 2010 prepared by Behera et al. [25]. Both the LULC maps have a spatial resolution of 170 m, with an overall classification accuracy greater than 91%, and thus these maps were suitable for studying the hydrologic impacts of LULC changes in IGRB. The VIC model typically divides each grid into $(n + 1)$ tiles, where n denotes the number of vegetation classes. The fractional coverage of n tiles is typically specified in the model, while the fractional coverage of the $(n + 1)$ th tile, which is assumed to be bare, is estimated by subtracting the sum of the fractions of the n vegetation tiles from 1 [27]. In this study, the fraction of each vegetation class, including evergreen broad-leaved forest, evergreen needle-leaved forest, deciduous forest, mixed forest, mangroves,

agriculture, scrubland and grassland were defined within the grid cell. Degraded forest and plantation were merged with the adjoining forest type. The non-vegetation classes, including waterbody, built-up, wasteland, and snow and ice, were not included in the vegetation parameter file of the VIC model and were therefore considered as bare [5, 27]. The effect of snow and ice and of water can be considered in the model by activating the snow and lake sub-models, respectively [27]. In previous applications of the VIC model, either the built-up class was classified as bare or the other LULC classes were rescaled to eliminate the built-up area. Therefore, built-up areas were not well represented. A simple bulk parameterization approach was employed in the present study to mimic the built-up area [33]. A hypothetical soil class was assigned to the grids that were dominated by the built-up class ($\geq 70\%$). The maximum allowable soil moisture was set to a minimum possible value for the assigned soil class to mimic the impervious surface associated with built-up areas. The wasteland class was assumed to be equivalent to bare ground in the present study.

Vegetation properties, primarily the monthly LAI, albedo, roughness length, displacement height, minimum stomatal resistance and architectural resistance, need to be defined in the model. The water balance is most sensitive to the LAI, among all the parameters. In the present study, we utilized the Moderate Resolution Imaging Spectroradiometer (MODIS) LAI data product MCD15A3 for 2010 and the LULC map of 2010 to extract the monthly LAI for each vegetation class. First, MODIS quality assurance (QA) information was used to extract cloud-free and best-quality pixels (Fig. 2). Homogeneous patches of each LULC class were then identified from the LULC map of 2010 using a moving window of size $1 \text{ km} \times 1 \text{ km}$. Finally, the quality pixels of the LAI imagery were selected

only if they fell within homogeneous LULC patches. This process was repeated for each month of 2010.

The other vegetation parameters, such as the albedo, roughness length, displacement height, minimum stomatal resistance and architectural resistance, were taken from Global Land Data Assimilation System (GLDAS) as described by Rodell et al. [34]. The GLDAS data set has been used successfully for Indian river basins [31, 35]. The vegetation parameters of each LULC do not change from year to year in this implementation of the VIC model [5, 21].

The values of daily meteorological variables, i.e., precipitation, at 0.5° resolution, and maximum and minimum temperatures, at 1° resolution, for the period from January 1971 to December 2005 developed by the Indian Meteorological Department (IMD) were used to force the VIC model.

3.3 Model Calibration and Evaluation

Calibration of the VIC model typically includes tuning soil parameters by analysing the agreement between the simulated and observed streamflows to improve the simulated hydrological fluxes. Since the part of the GRB excluded from the study also contributes to the main streams of the GRB, calibration of the model was not possible at these streams. Therefore we developed the set of calibrated soil parameters from two sub-catchments of the adjoining basin, i.e., the Mahanadi river basin. The outlets of these sub-catchments are at Sundergarh and Basantpur, as shown in Fig. 1. These sub-catchments have very similar soil characteristics as IGRB. Therefore, the set of soil parameters that has been developed can be used for IGRB. This technique of model calibration is very common in ungauged watersheds [36]. The VIC-simulated monthly streamflow from 2001 to 2010 were compared with the streamflow observed by the Central Water Commission (CWC), India, which are available at India-WRIS (<http://www.india-wris.nrsc.gov.in/>). The Nash–Sutcliffe efficiency (E_f) was used to evaluate the simulation accuracy, calculated as

$$E_f = 1 - \frac{\sum_{i=1}^N (Q_{mod,i} - Q_{obs,i})^2}{\sum_{i=1}^N (Q_{obs,i} - \overline{Q_{obs}})^2}, \quad (5)$$

where $Q_{mod,i}$ is the modelled streamflow for month i , $Q_{obs,i}$ is the observed streamflow for month i , N is the number of months, and $\overline{Q_{obs}}$ is the mean of the monthly observed streamflows. The VIC model performed reasonably, as seen from a comparison of the simulated and observed streamflows at Sundergarh and Basantpur (Fig. 3a, b).

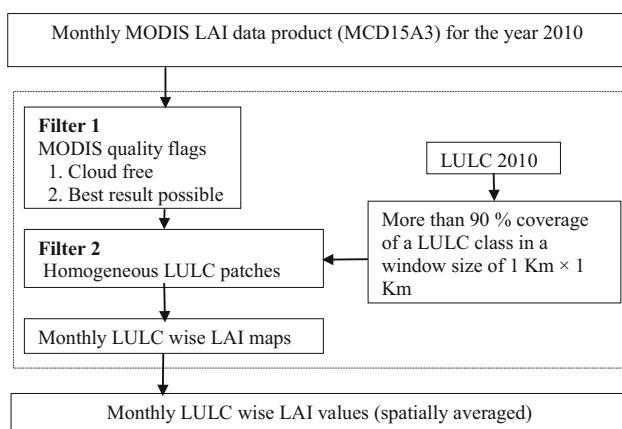
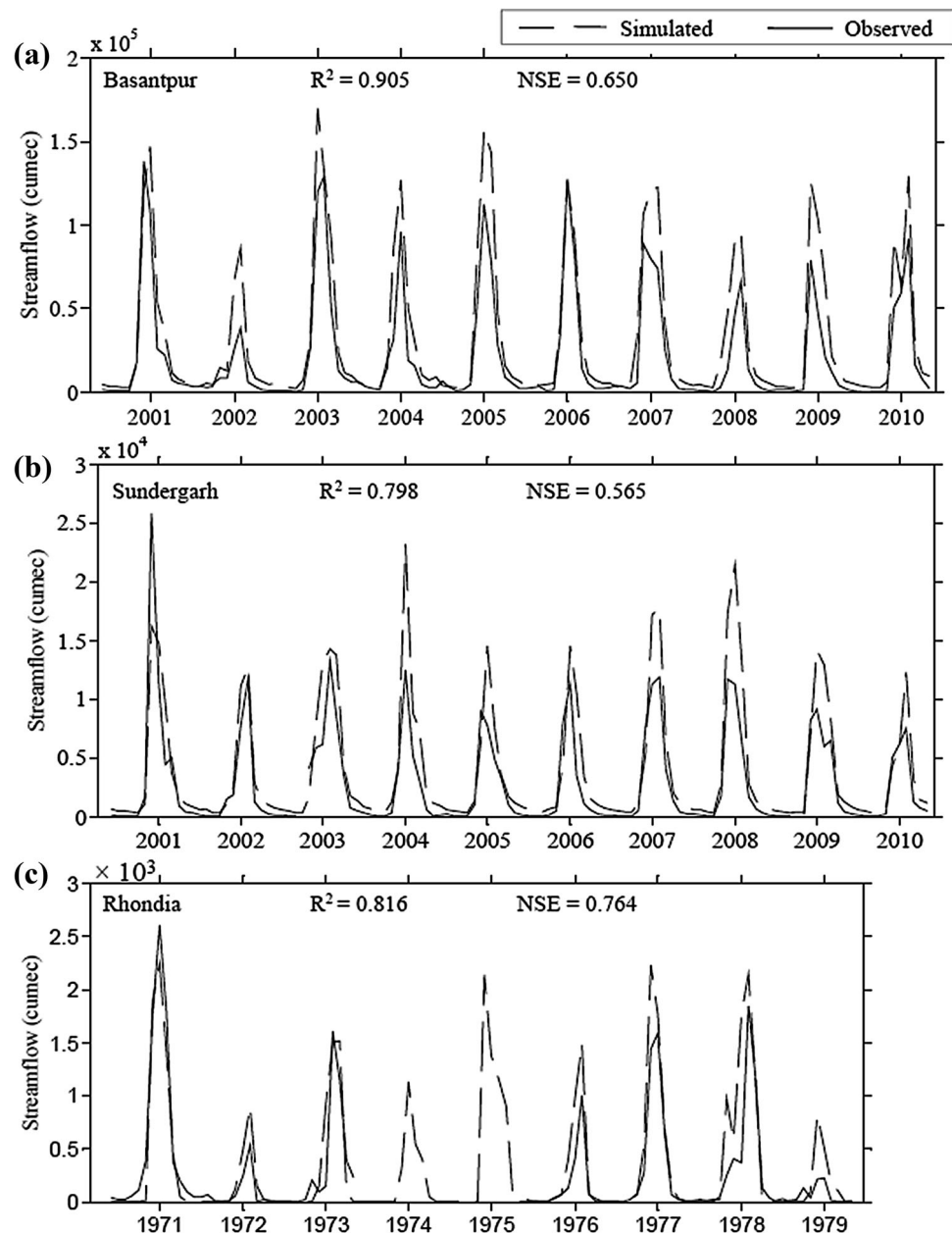


Fig. 2 Flowchart of methodology for monthly leaf area index (LAI) extraction using MODIS LAI data product MCD15A3

Fig. 3 Monthly simulated streamflow compared with observed streamflow at Basantpur (a), and Sundergarh (b) from January 2001 to December 2010, and at Rhondia (c) from January 1971 to December 1979



The Nash–Sutcliffe efficiencies (E_f) for these subcatchments were 0.565 and 0.650, respectively. Slight over-estimation was observed in the model-simulated streamflow. This might be the effect of bias in the observed streamflow due to dam management in the sub-basins. The calibrated soil parameters are shown in Table 1. In order to evaluate the performance of the model in IGRB, the streamflow simulated by the calibrated VIC model was compared with the observed streamflow of the river Damodar at Rhondia, in the GRB (Figs. 1a, 3c). The Nash–Sutcliffe efficiency of the model is 0.764 at the monthly scale, which is an acceptable value. Therefore, the set of

calibrated parameters was suitable for assessing the hydrologic impacts of LULC changes in IGRB.

4 Results and Discussion

4.1 LULC Changes in IGRB

The LULC maps of 1975 and 2010 of IGRB developed by Behera et al. [25] were analysed to explore grid-wise LULC changes and the associated hydrologic impacts. The LULC classes of the original LULC maps were simplified to four LULC classes, including forest, agriculture,

Table 1 Calibrated soil parameters

Parameter	Description	Calibrated value	Bounds
$b_{infiltr}$	Parameter used to describe the variable infiltration curve	0.1	10^{-5} to 0.4
D_s	Fraction of maximum velocity of base flow where non-linear base flow begins	0.1	Less than 1
W_s	Fraction of maximum soil moisture where nonlinear base flow occurs	0.75	Greater than 0.5
D_1, D_2	Soil layer thicknesses	$D_1 = 0.8$ m, $D_2 = 0.6$ m	0.1–1.5 m

scrubland/grassland and built-up for clarity in the LULC change map (Fig. 1b). A histogram was generated for the percentage of grid cell area changed for each LULC class to explore the compensation effect. Analysis showed that in most of the grids the change was within $\pm 5\%$, with the peak close to 0%, indicating small-scale LULC changes in IGRB (grids with no change were not shown in histograms). The histograms of the vegetation classes, including forest, agriculture and scrubland/grassland, were perfectly symmetric, showing that decreases in vegetation classes were significantly compensated by increases in these classes. In contrast to this, the histogram of built-up was skewed left, with the peak close to 0%. Built-up changed the most among all the LULC classes, increasing to 43% more than what it was in 1975. This indicates a significant expansion over the total built-up area of 1975. However, the expansion of the built-up class is less significant compared with the total geographical area of IGRB, i.e., an increase of 0.65%. This indicates that the LULC change was more pronounced at the local scale compared with the basin scale in IGRB due to the dominance of agriculture ($\sim 73\%$). At the basin scale, the negative LULC changes were compensated by positive LULC changes. For instance, an increase in forest due to plantation and regeneration of degraded forests was observed at some places; at the same time, conversion of forest to scrubland/wasteland or agriculture led to declines in forest at other places in the basin.

4.2 Sensitivity of LULC Change to ET and Runoff in IGRB

Understanding the mechanism of the hydrologic impacts of LULC changes is essential for sustainable management of water resources. The single-cell sensitivity analysis used in the present study provides the necessary basis for exploring and quantifying LULC change-induced changes in hydrological fluxes. Previous studies have successfully quantified the responses of hydrological components to LULC changes using single-cell sensitivity analysis in a variety of river basins of the world [5, 15, 21]. IGRB, however, has a substantially different climate due to its monsoon-

dominated rainfall. A grid cell located at $23^\circ 15' 1''N$ and $83^\circ 14' 59''E$ was selected. Continuous daily simulations for the period from 1971 to 2005 were performed in the selected grid cell by sequentially forcing the VIC model with 100% coverage of each LULC class while keeping all other variables unchanged. The average monthly ET and runoff were calculated and compared for each LULC class.

The monthly LAI derived from MODIS MCD15A3 was able to capture the phenological characteristics of different LULC types (Fig. 4a). Evergreen broad-leaved forest has the highest LAI among all the LULC classes (range 4–4.35), followed by evergreen needle-leaved forest (3.8–4.2), throughout the year. Evergreen forests (including evergreen broad-leaved forest and evergreen needle-leaved forest), as the name indicates, exhibit little variation in phenology through the year, and thus there was little variation in the monthly LAI.

Deciduous forest had significantly lower LAI values compared with evergreen forests during March–May, with the lowest value of 1.03 being for May and the highest value of 4.16 being for October. Mixed forest and mangroves had lower LAI values during March–May compared with evergreen forests, but these were higher than the values of deciduous forest. The LAI values of mixed forest and mangroves varied from 2.45 (in June) to 4.2 (September) and from 1.39 (May) to 3.9 (September), respectively. Agriculture had the highest LAI value of 4.24 in August and the lowest value of 0.87 in April. Scrubland had slightly higher LAI values compared with grassland throughout the year. The LAI values of scrubland varied from 0.6 (April) to 3.2 (September). The LAI values of grassland varied from 0.47 (April) to 2.3 (October). Overall, most of the LULC classes had their peak LAI values during the monsoon (June–September). The LAI values started declining in winter (October–January) and were lowest in summer (February–May). The MODIS-derived LAI values characterized the seasonal growth patterns of all the LULC classes appropriately, and there was a clear distinction between LULC classes. Thus the LAI values extracted were suitable for parameterizing the VIC model for LULC change analysis.

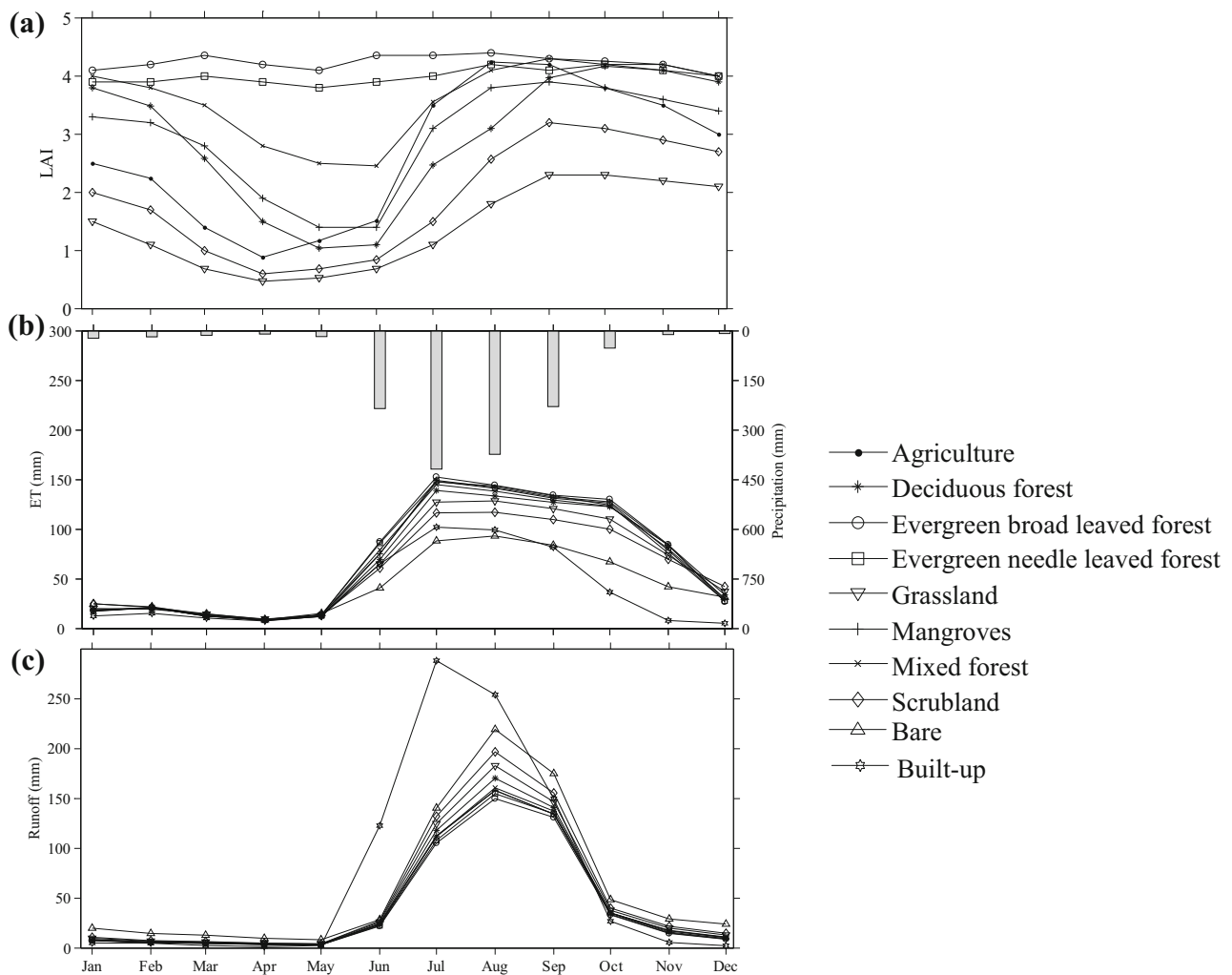


Fig. 4 Monthly Leaf Area Index (LAI) derived from MODIS LAI data product MCD15A3 (a), average (1971–2005) monthly precipitation and ET (b), and runoff (c) simulated from single cell sensitivity analysis

The analysis showed that the ET and runoff were considerably affected by the LAI and the water available to the plants for transpiration. The precipitation fluctuates significantly throughout the year, with most of it (> 70%) being received during the Indian summer monsoon, which typically begins in June, and the monsoon withdraws in September. In the grid cell selected for the sensitivity analysis, the precipitation was highest (394 mm) in month July, followed by August (352 mm) and September (216 mm) (Fig. 4b). The remaining months of the year were relatively dry (less than 48 mm/month).

The changes in the VIC-simulated ET and runoff values are mainly governed by changes in the properties of the vegetation, specifically the LAI, displacement height, roughness height and absence/presence of canopy. The LAI is the most sensitive vegetation parameter for ET and runoff among the parameters defined in the VIC model [27, 37]. Therefore LULC classes with higher LAI values

typically have higher ET and lower runoff values. In the present analysis, interclass variations in LAI were clearly reflected in the ET responses during the monsoon and winter (Fig. 4b). Both agriculture and forest classes, including evergreen needle-leaved forest, evergreen broad-leaved forest, mixed forest, mangroves and deciduous forest, had very similar ET values, which were the highest among all the LULC classes for the period from July to October. Each of the remaining LULC classes (scrubland, grassland, built-up and bare ground) had significantly different ET values compared with other LULC classes for the same period. The bare ground and built-up classes had the lowest ET values among all the classes, followed by grassland and scrubland. The ET responses during the summer were significantly different from those during the monsoon and winter, primarily due to limited availability of soil moisture. In November, the ET values started decreasing in all the LULC classes and converged to

Table 2 Hydrologic impact matrix generated from single cell sensitivity analysis, showing sensitivity of LULC change to annual ET and runoff (shown in parentheses) in mm

	EBF	ENF	MG	AG	MF	DDF	GL	SL	BARE	BU	Annual
EBF	0 (0)	- 21 (21)	- 22 (22)	- 32 (32)	- 34 (34)	- 51 (51)	- 94 (93)	- 134 (133)	- 302 (242)	- 377 (377)	836 (490)
ENF	21 (- 21)	0 (0)	- 1 (1)	- 12 (11)	- 14 (14)	- 30 (30)	- 73 (73)	- 113 (113)	- 281 (221)	- 356 (356)	815 (510)
MG	22 (- 22)	1 (- 1)	0 (0)	- 10 (10)	- 12 (12)	- 29 (29)	- 72 (72)	- 112 (111)	- 280 (220)	- 355 (355)	814 (512)
AG	32 (- 32)	12 (- 11)	10 (- 10)	0 (0)	- 2 (2)	- 18 (19)	- 62 (61)	- 102 (101)	- 270 (220)	- 345 (345)	803 (522)
MF	34 (- 34)	14 (- 14)	12 (- 12)	2 (- 2)	0 (0)	- 16 (16)	- 60 (59)	- 100 (99)	- 268 (207)	- 343 (343)	801 (524)
DDF	51 (- 51)	30 (- 30)	29 (- 29)	18 (- 19)	16 (- 16)	0 (0)	- 43 (43)	- 83 (83)	- 252 (191)	- 327 (326)	785 (540)
GL	94 (- 93)	73 (- 73)	72 (- 72)	62 (- 61)	60 (- 59)	43 (- 43)	0 (0)	- 40 (40)	- 208 (148)	- 283 (284)	742 (583)
SL	134 (- 133)	113 (- 113)	112 (- 111)	102 (- 101)	100 (- 99)	83 (- 83)	40 (- 40)	0 (0)	- 168 (108)	- 243 (244)	702 (623)
BARE	302 (- 242)	281 (- 221)	280 (- 220)	270 (- 209)	268 (- 207)	252 (- 191)	208 (- 148)	168 (- 108)	0 (0)	- 75 (135)	534 (731)
BU	377 (- 377)	356 (- 356)	355 (- 355)	345 (- 345)	343 (- 343)	327 (- 326)	283 (- 284)	243 (- 244)	75 (- 135)	0 (0)	548 (866)

EBF evergreen broad leaved forest, ENF evergreen needle leaved forest, MG mangroves, AG agriculture, MF mixed forest, DDF deciduous forest, GL grassland, SL scrubland, BARE bare ground, BU built-up

similar values from December to May. The VIC model includes a soil moisture limiting factor (g_{sm}) in the estimation of ET (as discussed in Sect. 3.1). g_{sm} increases linearly as the soil moisture content decreases, making the model more sensitive to it than to LAI. Thus, very similar ET responses were observed in all the LULC classes during the water-stressed period.

The VIC-simulated runoff of each grid cell is the residual of the water balance of that grid cell. Therefore the runoff responses in each LULC type were opposite to the ET responses (Fig. 4c). In the study area, the runoff is mainly driven by precipitation. Hence, during the monsoon significantly greater runoff was generated compared with the non-monsoon seasons. The greatest runoff values were observed in the built-up class, followed by bare ground, scrubland and grassland, throughout the year (except October–December), primarily due to lower infiltration and water loss through ET. The runoff from the built-up class was lowest during October–December, due to relatively low base flow generation as a result of the limited soil moisture storage capacity. The higher ET from the forest and agriculture classes led to lower runoff during the wet season. During the dry period, similar runoff values were observed for all the LULC classes, mainly due to their similar ET responses.

In order to understand the effects of LULC changes on the annual ET and runoff in IGRB, a hydrologic impact matrix was derived from the simulated fluxes of the single-cell sensitivity analysis (Table 2). Conversion from the evergreen broad-leaved forest class to the built-up class had the greatest impact on ET (decrease of 377 mm) and runoff (increase of 377 mm). The least impact was observed from the conversion of evergreen broad-leaved forest to evergreen needle-leaved forest, with a slight decrease in ET (21 mm) and increase in runoff (21 mm). The transformations among the classes, including evergreen needle-leaved forest, evergreen broad-leaved forest, mixed forest, mangroves, deciduous forest and agriculture, led to relatively small changes in the ET (ranging from 2 to 51 mm) and runoff (ranging from 2 to 51 mm). In contrast, conversion from forest or agriculture to scrubland, grassland, bare ground or built-up significantly altered the ET (ranging from 94 to 377 mm) and runoff (ranging from 93 to 377 mm).

The single-cell sensitivity analysis illustrates the responses of different LULC classes in terms of changes in the ET and runoff. From the analysis, it can be inferred that, hydrologically the most important LULC change in IGRB is conversion of the vegetation class to the built-up class. In contrast to this, conversion among forest classes and agriculture may have little effects on the ET and runoff. The interclass variability of the monthly LAI is high during the dry period, but the LAI changes the ET and

runoff relatively little during this period, mainly due to the limited soil moisture content. This leads to low interclass variations of the ET and runoff during the period. In contrast, there was relatively little interclass variation in the LAI during the wet season, when plenty of soil moisture is available to the plants. As a result, the hydrological fluxes in IGRB are less influenced by conversions among vegetation classes. Wagner et al. [11] also concluded that LULC changes may be less significant in this region, where the water availability is seasonally limited.

4.3 Impacts of LULC Changes on ET and Runoff at Basin and Sub-basin Scales

The effects of LULC changes on the ET and runoff in IGRB were analysed on an annual time scale. A delta approach was employed to assess the hydrologic impacts of LULC changes. In which two separate simulations of the VIC model were performed using LULC maps of 1975 and 2010, respectively, with the same climatic record (1971–2005) with a daily time step. This method of assessing the hydrologic impacts of LULC changes does not deliver results that reflect the hydrologic observations of the past decades. However, it illustrates the hydrologic impacts of LULC changes [11, 38]. The average annual ET and runoff were estimated on the basis of continuous simulations for 35 years (1971–2010). The simulated annual average ET and runoff maps of two LULC situations were then compared to explore the spatial pattern of changes and to assess the hydrologic impacts of LULC changes between 1975 and 2010. Changes in the annual ET and runoff caused by LULC change in the study area were observed in many of the model grids (Fig. 5a, b). The changes in the annual average ET ranged from an increase of 74 mm to a decrease of 123 mm within the model grids.

The opposite impact was observed on the runoff for all the grids, and these changes ranged from an increase of 122 mm to a decrease of 73 mm.

At the basin scale, the negative impacts were compensated by positive impacts. Therefore, net change in the annual hydrological fluxes was found to be insignificant (~ 1 mm). However, the impact was more pronounced at the local scale. Histograms of the percentage changes in the ET and runoff were generated to explore the compensation effect (Fig. 6).

The histograms of both the ET and runoff were perfectly symmetric, with the peak close to zero (note that grids with no change were not included in the histograms). Also, the changes in most of the model grids were within a range of $\pm 4\%$. A decrease in the ET was observed at some places in IGRB, primarily due to the conversion of forest or agriculture to wasteland, built-up or scrubland. In contrast, increases in ET were observed at other places, primarily due to increases in plantation and agriculture areas. Therefore, the increase in ET cancelled out the decrease in ET at the basin scale. The impacts of LULC changes were also analysed at sub-basin scale. The results show that the changes are more pronounced at sub-basin level. Figures 7a, b show the change in annual ET and runoff per sub-basin in mm. The changes in annual ET range from a decrease of -8.5 mm to an increase of 9.2 mm. Whereas the changes in annual runoff range from a decrease of -9.2 mm to an increase of 8.4 mm. The analyses shows that the small sub-basins are more sensitive to LULC changes due to less compensation effect.

Ashagrie et al. [13] also found that the overall hydrologic impacts of LULC changes may be too small to be detected at the basin scale. Recently, Wagner et al. [11] studied the impacts of LULC changes in the catchment of the Mula and Mutha rivers upstream of Pune, India. They

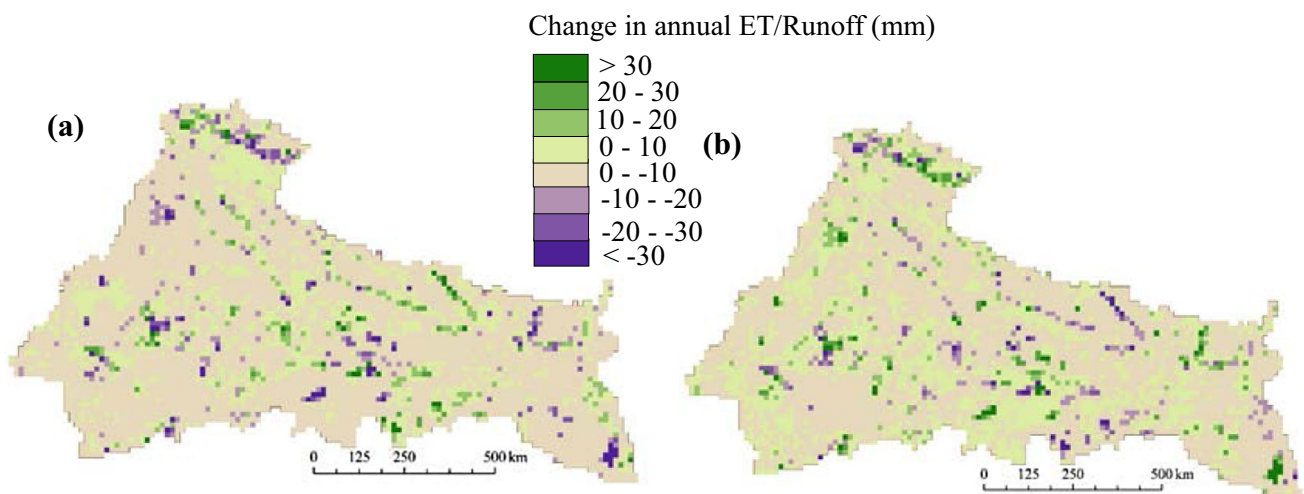


Fig. 5 Annual average hydrologic response differences between 1975 and 2010, ET (a), and runoff (b)

Fig. 6 Histograms of change in LULC (a), and change in hydrological fluxes (b) within grid cells of resolution 0.125°

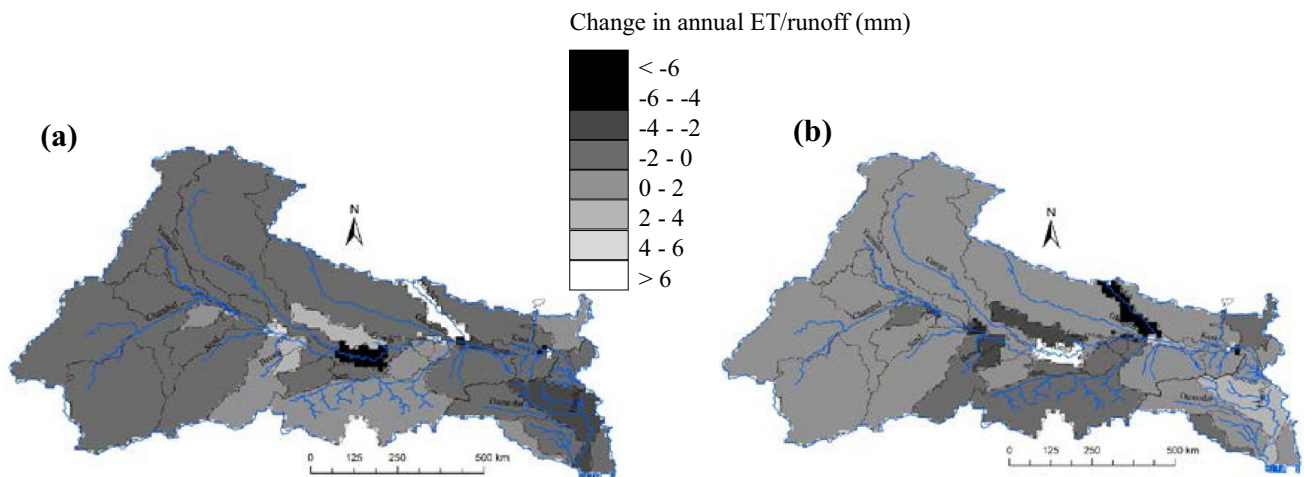
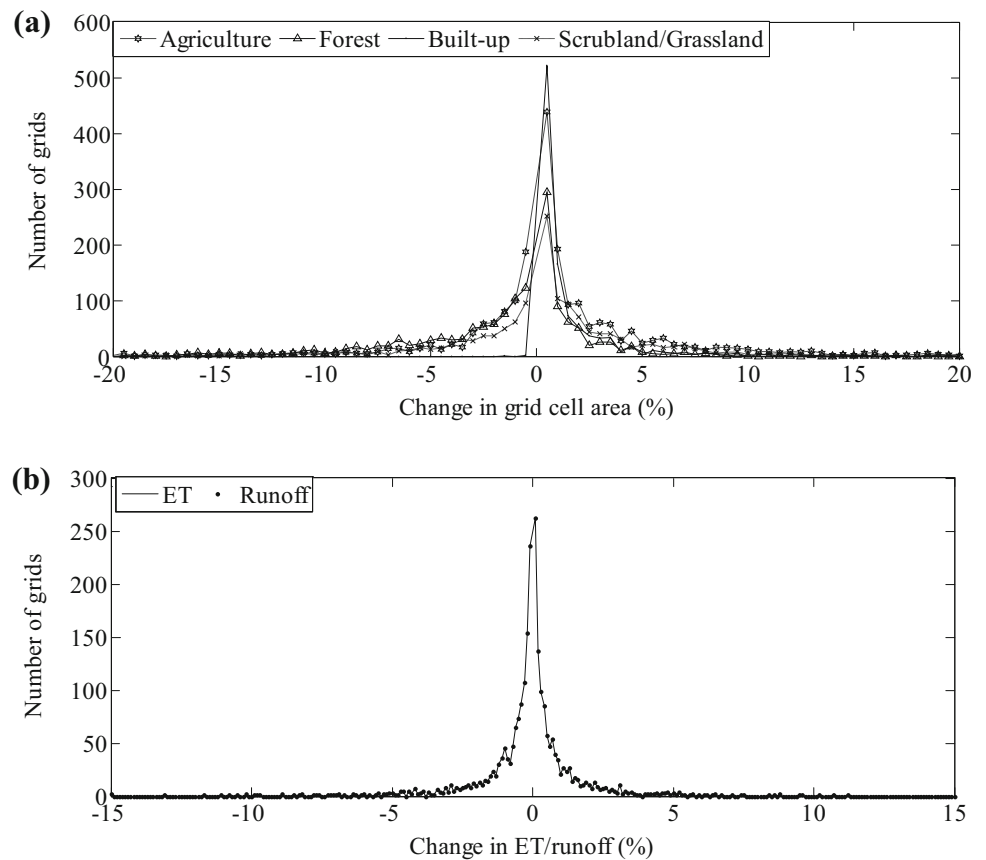


Fig. 7 Annual average hydrologic response differences between 1975 and 2010 at sub-basin scale, ET (a), and runoff (b)

found that the impacts were too small at the basin scale due to compensation effects, even after substantial LULC changes. In this study, we found that the impacts on the ET and runoff were cancelled out at the basin scale; however, they could be observed at the local scale. Also, the LULC changes that have taken place in IGRB during the last 35 years (1975–2010) are too small to make significant changes in the ET and runoff.

4.4 Limitations of the Study

The impacts of LULC changes on ET and runoff were assessed utilizing VIC simulated ET and runoff. The VIC model is a physically based distributed model and therefore less sensitive to the model calibration. Hurkmans et al. [39] compared VIC model with STREAM and found that the performance of VIC is more robust with less requirement

of model calibration. In this study, we attempt to calibrate the VIC model on Mahanadi river basin as the river discharge data for the study area was not available. A more reliable scenario of hydrologic impacts of LULC changes could be derived if the model was calibrated and validated on the study area as the soil variability in the study area is higher than Mahanadi river basin.

The single-cell sensitivity analysis used in the present study provides the necessary basis for exploring and quantifying LULC change-induced changes in hydrological fluxes. However, it should be noted that the sensitivity of ET and runoff to LULC changes might be different in different model grids in the study area from those found in single-cell sensitivity analysis due to variability in soil, precipitation, temperature and land slope.

5 Conclusions

Urbanization and expansion of agriculture were the most important LULC changes during the past three decades in IGRB. The analysis showed that replacement of vegetation by built-up land is the change that affected the water balance of the IGRB most. Conversions among forest classes and conversion from forest to agriculture may not affect the water balance significantly. The effects of LULC changes are more pronounced during the monsoon. However, the limited availability of soil moisture during the dry season leads to similar ET and runoff responses from most of the LULC classes. The overall changes in hydrological fluxes due to LULC changes in IGRB during the study period were found to be insignificant at the basin scale, and this is a positive sign in the basin. We observed that the ET and runoff were altered significantly with LULC changes; however, at the basin scale, the negative impacts were cancelled by the positive impacts. While one part of the basin experiencing changes from higher ET/runoff to lower ET/runoff due to LULC conversion, the other part may be experiencing the opposite. The impacts of LULC changes were not as intense as those found in most other river basins of the world. These were primarily due to three reasons: (1) the small scale of LULC changes in IGRB, (2) compensation of negative impacts by positive impacts in the basin and (3) seasonally limited water availability.

References

- Boulain N, Cappelaere B, Séguis L et al (2009) Water balance and vegetation change in the Sahel: a case study at the watershed scale with an eco-hydrological model. *J Arid Environ* 73:1125–1135. <https://doi.org/10.1016/j.jaridenv.2009.05.008>
- Chahine TM (1992) The hydrological cycle and its influence on climate. *Nature* 359:373–379
- Turner BL, Matson PA, McCarthy JJ et al (2003) Illustrating the coupled human-environment system for vulnerability analysis: three case studies. *Proc Natl Acad Sci USA* 100:8080–8085. <https://doi.org/10.1073/pnas.1231334100>
- Pielke RA, Avissar R (1990) Influence of landscape structure on local and regional climate. *Landsc Ecol* 4:133–155
- Mao D, Cherkauer KA (2009) Impacts of land-use change on hydrologic responses in the Great Lakes region. *J Hydrol* 374:71–82. <https://doi.org/10.1016/j.jhydrol.2009.06.016>
- Dadhwal VK, Aggarwal SP, Mishra N (2010) Hydrological simulation of mahanadi river basin and impact of land use/land cover change on surface runoff using a macro scale hydrological model. In: ISPRS TC VII Symposium—100 years ISPRS, Vienna, Austria XXXVIII, pp 165–170
- Mishra A, Kar S, Singh VP (2007) Prioritizing structural management by quantifying the effect of land use and land cover on watershed runoff and sediment yield. *Water Resour Manag* 21:1899–1913. <https://doi.org/10.1007/s11269-006-9136-x>
- Costa MH, Botta A, Cardille JA (2003) Effects of large-scale changes in land cover on the discharge of the Tocantins River, Southeastern Amazonia. *J Hydrol* 283:206–217. [https://doi.org/10.1016/S0022-1694\(03\)00267-1](https://doi.org/10.1016/S0022-1694(03)00267-1)
- Werth D, Avissar R (2002) The local and global effects of Amazon deforestation. *J Geophys Res* 107:8087. <https://doi.org/10.1029/2001JD000717>
- VanShaar JR, Haddeland I, Lettenmaier DP (2002) Effects of land-cover changes on the hydrological response of interior Columbia River basin forested catchments. *Hydrol Process* 16:2499–2520. <https://doi.org/10.1002/hyp.1017>
- Wagner PD, Kumar S, Schneider K (2013) An assessment of land use change impacts on the water resources of the Mula and Mutha Rivers catchment upstream of Pune, India. *Hydrol Earth Syst Sci* 17:2233–2246. <https://doi.org/10.5194/hess-17-2233-2013>
- Bloschl G, Ardoin-Bardin S, Bonell M et al (2007) At what scales do climate variability and land cover change impact on flooding and low flows? *Hydrol Process* 21:1241–1247. <https://doi.org/10.1002/hyp>
- Ashagrie AG, de Laat PJM, de Wit MJM et al (2006) Detecting the influence of land use changes on Floods in the Meuse River Basin—the predictive power of a ninety-year rainfall-runoff relation. *Hydrol Earth Syst Sci* 3:529–559. <https://doi.org/10.5194/hessd-3-529-2006>
- Iroumé A, Palacios H (2013) Afforestation and changes in forest composition affect runoff in large river basins with pluvial regime and Mediterranean climate, Chile. *J Hydrol* 505:113–125. <https://doi.org/10.1016/j.jhydrol.2013.09.031>
- Hurkmans RTWL, Terink W, Uijlenhoet R et al (2009) Effects of land use changes on streamflow generation in the Rhine basin. *Water Resour Res* 45:1–15. <https://doi.org/10.1029/2008WR007574>
- Claessens L, Hopkinson C, Rastetter E, Vallino J (2006) Effect of historical changes in land use and climate on the water budget of an urbanizing watershed. *Water Resour Res*. <https://doi.org/10.1029/2005WR004131>
- Dams J, Woldeamlak ST, Batelaan O (2008) Predicting land-use change and its impact on the groundwater system of the Kleine Nete catchment, Belgium. *Hydrol Earth Syst Sci* 12:1369–1385
- Fohrer N, Haverkamp S, Eckhardt K, Frede H-G (2001) Hydrologic response to land use changes on the catchment scale. *Phys Chem Earth B Hydrol Atmos* 26:577–582. [https://doi.org/10.1016/S1464-1909\(01\)00052-1](https://doi.org/10.1016/S1464-1909(01)00052-1)
- Hundecha Y, Bárdossy A (2004) Modeling of the effect of land use changes on the runoff generation of a river basin through

- parameter regionalization of a watershed model. *J Hydrol* 292:281–295. <https://doi.org/10.1016/j.jhydrol.2004.01.002>
20. Im S, Kim H, Kim C, Jang C (2009) Assessing the impacts of land use changes on watershed hydrology using MIKE SHE. *Environ Geol* 57:231–239. <https://doi.org/10.1007/s00254-008-1303-3>
 21. Mishra V, Cherkauer KA, Niyogi D et al (2010) A regional scale assessment of land use/land cover and climatic changes on water and energy cycle in the upper Midwest United States. *Int J Climatol* 30:2025–2044. <https://doi.org/10.1002/joc>
 22. Poelmans L, Van Rompaey A, Ntegeka V, Willems P (2011) The relative impact of climate change and urban expansion on peak flows: a case study in central Belgium. *Hydrol Process* 25:2846–2858. <https://doi.org/10.1002/hyp.8047>
 23. Quilbé R, Rousseau AN, Moquet J-S et al (2007) Hydrological responses of a watershed to historical land use evolution and future land use scenarios under climate change conditions. *Hydrol Earth Syst Sci Discuss* 4:1337–1367. <https://doi.org/10.5194/hessd-4-1337-2007>
 24. Liang X, Lettenmaier DP, Wood EF, Burges SJ (1994) A simple hydrologically based model of land surface water and energy fluxes for general circulation models. *J Geophys Res* 99:14415–14428. <https://doi.org/10.1029/94JD00483>
 25. Behera MD, Patidar N, Chitale VS et al (2014) Increase in agricultural patch contiguity over the past three decades in Ganga River Basin, India. *Curr Sci* 107:502–511
 26. Raju BMK, Rao KV, Venkateswarlu B et al (2013) Revisiting climatic classification in India: a district-level analysis. *Curr Sci* 105:492–495
 27. Gao H, Tang Q, Shi X et al (2009) Water budget record from variable infiltration capacity (VIC) model algorithm theoretical basis document. Dept. Civ. Environ. Eng. Univ, Seattle
 28. Lohmann D, Raschke E, Nijssen B, Lettenmaier DP (1998) Regional scale hydrology: I. formulation of the VIC-2L model coupled to a routing model. *Hydrol Sci J* 43:131–141. <https://doi.org/10.1080/02626669809492107>
 29. Dickinson RE, Henderson-Sellers A, Rosenzweig C, Sellers PJ (1991) Evapotranspiration models with canopy resistance for use in climate models, a review. *Agric For Meteorol* 54:373–388. [https://doi.org/10.1016/0168-1923\(91\)90014-H](https://doi.org/10.1016/0168-1923(91)90014-H)
 30. Franchini M, Pacciani M (1991) Comparative analysis of several conceptual rainfall-runoff models. *J Hydrol* 122:161–219
 31. Aggarwal SP, Garg V, Gupta PK et al (2013) Run-off potential assessment over Indian landmass: a macro-scale hydrological modelling approach. *Curr Sci* 104:950–958. <https://doi.org/10.1029/2000JD000146.7>
 32. Cosby BJ, Hornberger GM, Clapp RB, Ginn TR (1984) A statistical exploration of the relationships of soil moisture characteristics to the physical properties of soils. *Water Resour Res* 20:682–690. <https://doi.org/10.1029/WR020i006p00682>
 33. Yang G, Bowling LC, Cherkauer KA et al (2010) Hydroclimatic response of watersheds to urban intensity: an observational and modeling-based analysis for the white River Basin, Indiana. *J Hydrometeorol* 11:122–138. <https://doi.org/10.1175/2009JHM1143.1>
 34. Rodell M, Houser PR, Jambor U et al (2004) The global land data assimilation system. *Bull Am Meteorol Soc* 85:381–394. <https://doi.org/10.1175/BAMS-85-3-381>
 35. Raje D, Krishnan R (2012) Bayesian parameter uncertainty modeling in a macroscale hydrologic model and its impact on Indian river basin hydrology under climate change. *Water Resour Res*. <https://doi.org/10.1029/2011WR011123>
 36. Razavi T, Coulibaly P (2013) Streamflow prediction in ungauged basins: review of regionalization methods. *J Hydrol Eng* 10:958–975. [https://doi.org/10.1061/\(ASCE\)HE.1943-5584.0000690](https://doi.org/10.1061/(ASCE)HE.1943-5584.0000690)
 37. Matheussen B, Kirschbaum R, Goodman I et al (2000) Effects of land cover change on streamflow in the interior Columbia River Basin (USA and Canada). *Hydrol Process* 14:867–885
 38. Miller SN, Kepner WG, Mehaffey MH et al (2002) Integrating landscape assessment and hydrologic modeling for land cover change analysis. *Jawra* 38:915–929. <https://doi.org/10.1111/j.1752-1688.2002.tb05534.x>
 39. Hurkmans RTWL, De Moel H, Aerts JCJH, Troch PA (2008) Water balance versus land surface model in the simulation of Rhine river discharges. *Water Resour Res* 44:1–14. <https://doi.org/10.1029/2007WR006168>